Lack of EP4 receptors on bone marrow-derived cells enhances inflammation in atherosclerotic lesions

Eva H.C. Tang[1,2], Koichi Shimizu[1], Thomas Christen[1], Viviane Z. Rocha[1], Eugenia Shvartz[1], Yevgenia Tesmenitsky[1], Galina Sukhova[1], Guo-Ping Shi[1], and Peter Libby[1]*

[1]Division of Cardiovascular Medicine, Brigham and Women's Hospital, Harvard Medical School, 77 Avenue Louis Pasteur, NRB741, Boston, MA 02115, USA; and [2]Department of Pharmacology and Pharmacy, The University of Hong Kong, 21 Sassoon Road, 2/F Li Ka Shing Faculty of Medicine, Faculty of Medicine Building, Hong Kong SAR, China

Aim	Prostaglandin E$_2$, by ligation of its receptor EP4, suppresses the production of inflammatory cytokines and chemokines in macrophages *in vitro*. Thus, activation of EP4 may constitute an endogenous anti-inflammatory pathway. This study investigated the role of EP4 in atherosclerosis *in vivo*, and particularly its impact on inflammation.
Methods and results	Ldlr$^{-/-}$ mice transplanted with EP4$^{+/+}$ or EP4$^{-/-}$ bone marrow consumed a high-fat diet for 5 or 10 weeks. Allogenic bone marrow transplantation promoted exacerbation of atherosclerosis irrespective of EP4 genotype, compatible with prior observations of exacerbated atherogenesis by allogenicity. EP4 deficiency had little effect on plaque size or morphology in early atherosclerosis, but at the later time point, mice deficient in EP4 displayed enhanced inflammation in their atherosclerotic plaques. Expression of monocyte chemoattractant protein-1 and interferon-γ inducible protein 10 increased, and there was a corresponding increase in macrophage and T-cell infiltration. These plaques also contained fewer smooth muscle cells. Despite these changes, mice deficient in EP4 in bone marrow-derived cells at an advanced stage had similar lesion size (in both aorta and aortic root) as mice with EP4.
Conclusion	This study shows that in advanced atherosclerosis, EP4 deficiency did not alter atherosclerotic lesion size, but yielded plaques with exacerbated inflammation and altered lesion composition.
Keywords	E prostanoid receptor 4 • EP4 receptor • Inflammation • Atherosclerosis • Atherogenesis

1. Introduction

In atherosclerosis, a chronic inflammatory disease, the balance between persistent pro-inflammatory signals and intrinsic anti-inflammatory pathways influences the development, progression, and clinical manifestation of atherosclerotic plaques. In response to various stimuli, the sequential actions of cyclooxygenase and prostaglandin E synthase produce prostaglandin E$_2$ (PGE$_2$) from arachidonic acid.[1] PGE$_2$ elicits a range of biological effects via its interaction with E prostanoid (EP) receptors. EP1, EP2, EP3, and EP4—seven-transmembrane G-protein-coupled receptors—comprise the four subtypes of EP receptors.[1]

PGE$_2$ inhibits the release of a number of cytokines and chemokines *in vitro*. In human macrophages, PGE$_2$ attenuated lipopolysaccharide (LPS)-induced mRNA and protein expression of chemokines, including monocyte chemoattractant protein-1 (MCP-1), interferon-γ inducible protein 10 (IP-10), interleukin-8, macrophage inflammatory protein-1α, and macrophage inflammatory protein-1β.[2,3] PGE$_2$ also inhibited tumor necrosis factor-α, IFNγ, and interleukin-1β-mediated expression of these chemokines.[2] Interestingly, suppression by PGE$_2$ of chemokine expression occurred in macrophages, but not in activated endothelial cells and smooth muscle cells (SMC).[2] EP4 mediates these anti-inflammatory effects of PGE$_2$.[2,3]

The action of the receptor EP4 depends characteristically on transiently increased intracellular cAMP via the G protein, Gα. cAMP activates protein kinase A (PKA), which then phosphorylates downstream effector proteins, such as cAMP response element-binding protein.[4] But chemokine suppression by PGE$_2$ in

macrophages involves a mechanism independent of this classic pathway. Instead, a protein called EP4 receptor-associated protein associates with the long carboxyl terminal cytoplasmic domain of EP4, enhances the stability of p105 (an important cytoplasmic inhibitor of NFκB and MEK activation), and attenuates NFκB and MEK activation.[5,6]

The EP4-dependent suppression by PGE$_2$ of chemokine production in macrophages, leading to reduced infiltration of inflammatory cells, renders the receptor EP4 a possible therapeutic target to treat inflammatory disease. Indeed, an EP4 agonist effectively reduced acute cardiac rejection and prolonged allograft survival in mice by suppressing myocardial inflammation.[6] EP4 agonists also protected reperfused myocardium from ischaemic injury by reducing inflammation.[7,8] Mice lacking EP4 on their haematopoietic cells exhibited greater local inflammation and an increased prevalence of abdominal aortic aneurysms.[9] Human atherosclerotic plaques display increased biosynthesis of PGE$_2$.[10,11] EP4 constitutes the predominant PGE$_2$ receptor isoform present in human macrophages, both in culture and in human atheroma.[2,10,11]

During the course of our study, Babaev et al. (2009)[12] showed that EP4 deficiency promoted macrophage apoptosis and suppressed early atherosclerosis. In their study, foetal liver cell transplantation generated Ldlr$^{-/-}$ mice chimeric for EP4$^{-/-}$ haematopoietic cells. This procedure involves genotyping foetuses and pooling foetal liver cells from multiple offspring, and chimeric mice generated by this method are histocompatible. In the study by Babaev et al., mice deficient in EP4 had reduced atherosclerosis compared with the wild-type mice after 8 weeks on a Western diet. The authors reasoned that the cause of reduction in plaque cellularity and volume in early atherosclerosis associated with augmented apoptosis of macrophages. Apoptosis may modulate the development of atherosclerotic lesions and plaque instability,[13–15] but its multifaceted effects depend greatly on the time point of the disease. In early atherosclerosis, neighbouring phagocytes rapidly clear apoptotic cells, a process called efferocytosis, which prevents secondary cellular necrosis and inflammation—thus, apoptosis could decrease lesion cellularity.[14,15] But in the setting of more advanced atherosclerosis, macrophage apoptosis and defective efferocytosis occur, and plaque necrosis, inflammation, and tissue damage ensue, promoting necrotic core formation.[14,15]

This study examined the role of EP4 in inflammation and its contribution to atherosclerosis in vivo. Clinical data indicate that cyclooxygenase-2 inhibitors may increase coronary events in some individuals.[16] Therefore, a more complete characterization of anti-inflammatory pathways stimulated by cyclooxygenase-2-dependent products may have considerable practical and clinical impact, in addition to pathophysiological interest.

2. Methods

2.1 Mice

Homozygous EP4 receptor-deficient (EP4$^{-/-}$) mice and wild-type (EP4$^{+/+}$) mice on the same genetic background were obtained by crossing mice heterozygous for ptger4 gene mutation (EP4$^{+/-}$) and verified as previously described.[17] Because EP4$^{-/-}$ mice only survive on a recombinant inbred strain, all EP4$^{-/-}$ and EP4$^{+/+}$ mice used in this study were on a mixed background, composed of 129/Olac, C57BL/6, and DBA/2.[17] Female 8-to-10-week-old Ldlr$^{-/-}$ (B6, 129S-Ldlr^{tm1Her}) mice on the C57BL/6 background were purchased from the Jackson Laboratory (Bar Harbor, ME, USA). All experiments conformed with the Guide for the Care and Use of Laboratory Animals, published by the U.S. National Institutes of Health (NIH Publication No. 85-23, revised 1996), and were performed under protocols approved by the Animal Research Committee of Harvard Medical School.

2.2 Bone marrow transplantation

Bone marrow transplantation was performed as described previously.[18] Bone marrow-derived cells from male donor EP4$^{+/+}$ or EP4$^{-/-}$ mice were obtained from their tibias and femurs and then injected (1 × 10^7 cells per mouse) into the tail vein of female Ldlr$^{-/-}$ recipient mice, which had been irradiated with 1000 rads from a Cesium source one day before injection. After 5 weeks of resting, chimeric mice with (EP4$^{+/+}$/ldlr$^{-/-}$) or without (EP4$^{-/-}$/ ldlr$^{-/-}$) EP4 haematopoietic cells were placed on a high-fat diet ad libitum (D12108 from Research Diets; 40% kcal from fat, 1.25% cholesterol). Subgroups were killed after 5 and 10 weeks on the diet. Successful reconstitution of recipients with cells of donor origin after bone marrow transplantation was established at the time of sacrifice by PCR-assisted amplification of wild-type and the EP4 null mutant gene. Semi-quantitative PCR analysis revealed that >90% of the bone marrow cells from EP4$^{-/-}$/ldlr$^{-/-}$ chimeras were of donor origin, indicating that bone marrow transfer was successful. Immunostaining of the aortic root for the presence of EP4 protein within the lesions further affirmed the success of the transplant.

2.3 Preparation of mouse aortae and quantification of atherosclerosis

On the day of harvesting, mice were anaesthetized by intraperitoneal injection with 2,2,2-tribromoethanol (2.5 mg/10 g body weight). The entire aorta (from the aortic root to the iliac bifurcation) was dissected out, cleaned of adhered fat, and fixed in 10% buffered formalin. They were then opened longitudinally and stained with Oil red O as previously described.[19,20] The extent of atherosclerosis was determined using the en face method, and expressed as positive Oil red O area over the total area of the whole aorta. Aortic roots were embedded in OCT, and sequential 6 μm frozen sections were made. The section with the largest cross-sectional lesion area from each individual mouse was stained with Oil red O, and lipid burden at the root was expressed as positive Oil red O area over lesion area. The size of aortic root lesions was expressed as lesion area over total lumen area.

2.4 Lipid analyses

Blood was collected by cardiac puncture using a needle with heparin. Plasma triglycerides and total cholesterol were determined using Infinity triglyceride or cholesterol lipid stable reagent (Thermo Scientific, Middletown, VA, USA).

2.5 Histological examination of lesion morphology

Frozen 6 μm sections were prepared and stained for EP4 (1:100; Cayman Chemicals, Ann Arbor, MI, USA), macrophages (Mac-3, 1:900; Pharmingen, San Diego, CA, USA), T cells (CD4, 1:100; Pharmingen), MCP-1 (1:50, Pharmingen), IP-10 (1:50; R&D Systems, Minneapolis, MN, USA), and SMC (α-actin, 1:75; Santa Cruz Biotech Inc., Santa Cruz, CA, USA), as described previously.[19–21] Lesional apoptotic cells were determined with the in situ apoptosis detection kit according to the manufacturer's instructions (Chemicon International, Temecula, CA, USA). CD4-positive cells and apoptotic cells in the intimal lesions were counted and expressed over lesion area. Other staining was analysed using the Image-Pro Plus program (Media Cybernetics, Silver Spring, MD, USA), and positive stained area in the intimal lesions was expressed over cross-section lesional area. Only positive staining within the lesions was included in quantification analysis. To localize EP4 protein to cell types, we used double fluorescent immunohistochemistry. Mouse cell type-specific

antibodies conjugated with fluorochrome—CD11b-APC (macrophage, Pharmingen) or CD3-PE (T cells, Pharmingen)—were mixed with rabbit anti-EP4 antibody. Staining for EP4 used goat anti-rabbit Alexa Fluora 488 (Invitrogen Molecular Probes). For colocalization of EP4 with SMC, after the first staining, sections underwent two blocking procedures: treatment with an avidin/biotin blocking kit (Vector Laboratories) according to the manufacturer's recommendations; and blocking with 5% appropriate normal serum for 20 min. Goat anti-mouse α-actin antibody (Santa Cruz) was followed by biotinylated anti-goat secondary antibody and streptavidin conjugated with FITC (Amersham).

2.6 Quantification of gene expression by reverse transcription-quantitative PCR

Total RNA was isolated with RNeasy tissue mini kit (Qiagen), and equal amounts were reverse-transcribed by Superscript II (Invitrogen), according to the manufacturer's instructions. Quantitative PCR was performed in a MyiQ Single Color Real-Time PCR Detection System (Bio-Rad). The following primers were used: IP-10, 5′-GCTGCCGTCATTTT CTGC-3′ and 5′-TCTCACTGGCCCGTCATC-3′; MCP-1, 5′-GGCTGG AGAGCTACAAGAGG-3′ and 5′-TCTTGAGCTTGGTGACAAAAA C-3′. The mRNA level of the genes tested was normalized to β-actin, used as an internal control in all experiments.

2.7 Echocardiography

Echocardiographs were conducted using the Visual Sonics Vevo 2100 echocardiograph machine with the MS550S 18–38 MHz transducer (Ontario, Canada). Animals were restrained briefly by the nape of the neck under 2% isoflurane, the heart was imaged in the two-dimensional parasternal short-axis view, and an M-mode measurement was recorded at the mid-ventricle at the level of the papillary muscle. The heart rate, end-diastolic, and end-systolic dimensions were measured from the M-mode image, and fractional shortening and ejection fraction were calculated using the Visual Sonics advanced cardiovascular package as an index of cardiac contractile function.

2.8 *In situ* zymography

Collagenolytic activity was determined on 6 μM frozen sections, using collagen conjugated with quenched fluorescein (DQ collagen; Invitrogen, Carlsbad, CA, USA) as a substrate, which requires cleavage by collagenolytic enzymes to become fluorescent. In brief, DQ collagen (1 mg/ml in H_2O) was mixed 1:10 with 1% low-melting agarose (Sigma-Aldrich, Milwaukee, WI, USA). This mixture (20 μl) was added on top of each section, coverslipped, and gelled at 4°C. Following incubation at 37°C for 48 h, fluorescence was examined using a fluorescent microscope. Cysteine protease activity was estimated using a pH 5.5 buffer containing EDTA (a chelator of calcium to inhibit MMP activity; 10 mM). MMP activity was evaluated using a pH 7.4 buffer containing E64 (a non-selective inhibitor of cysteine proteases; 20 μM).[20]

2.9 Statistical analysis

Data are expressed as mean $\pm$ SEM. All statistical analysis was performed using GraphPad Prism software 5.0 (San Diego, CA, USA). The two-tailed Mann–Whitney *t*-test was used for comparisons between experimental groups. Differences were considered statistically significant at $P < 0.05$.

3. Results

Five weeks after bone marrow transplantation, chimeric mice with or without EP4 bone marrow-derived cells consumed a high-fat diet for 5 or 10 weeks. No differences occurred in total plasma cholesterol, triglycerides, and body weight between EP4$^{+/+}$/ldlr$^{-/-}$ mice and EP4$^{-/-}$/ldlr$^{-/-}$ mice at either time point (*Table 1*). Semi-quantitative PCR analysis revealed that >90% of the bone marrow cells from EP4$^{-/-}$/ldlr$^{-/-}$ chimeras were of donor origin, indicating successful bone marrow transfer. Immunostaining of the aortic root for the presence of EP4 protein showed that EP4 localized most abundantly around the caps of the plaques (*Figure 1A*). Double immunofluorescent experiments show that both macrophages (*Figure 1C*) and T cells (*Figure 1D*) expressed EP4. Lesions of EP4$^{-/-}$/ldlr$^{-/-}$ mice contained EP4-positive staining, owing to host-derived EP4, but at levels ~50% lower than the amount found in EP4$^{+/+}$/ldlr$^{-/-}$ lesions (*Figure 1A* and *1B*); this trend occurred at both high-fat-fed time points. Co-localization of EP4 with α-actin demonstrates that the majority of the host-derived EP4 in the EP4$^{-/-}$/ldlr$^{-/-}$ lesions were SMC (*Figure 1E*).

EP4$^{+/+}$/ldlr$^{-/-}$ mice and EP4$^{-/-}$/ldlr$^{-/-}$ mice began to die at late stages of the study. At 10 weeks of a high-fat diet, EP4$^{+/+}$/ldlr$^{-/-}$ mice and EP4$^{-/-}$/ldlr$^{-/-}$ mice had survival rates of 80% (8 of 10) and 64% (7 of 11), respectively. Although mice deficient in EP4 appeared to have a lower survival rate, this did not reach statistical significance. The worsening in plaque characteristics in EP4-deficient mice was not reflected by a greater death rate, possibly because the study was not powered for a mortality endpoint.

Upon sacrifice of these mice for tissue harvest, we measured the wet weight of their hearts. Heart weight increased with time for both experimental groups, indicating remodelling of the heart. Heart weights did not differ between EP4$^{+/+}$/ldlr$^{-/-}$ mice and EP4$^{-/-}$/ldlr$^{-/-}$ mice at 5 weeks, but at 10 weeks, EP4$^{-/-}$/ldlr$^{-/-}$ mice had significantly heavier hearts than did EP4$^{+/+}$/ldlr$^{-/-}$ mice (*Figure 1F*). Because of the difference in heart mass, we performed echocardiograms on a separate cohort of mice to determine whether any corresponding change in heart function had occurred. At 5 weeks, the average fractional shortening in the hearts of EP4$^{+/+}$/ldlr$^{-/-}$ mice and EP4$^{-/-}$/ldlr$^{-/-}$ mice was 47.2 + 2.7% and 46.6 + 3.9%, respectively. At 10 weeks, fractional shortening in the hearts of EP4$^{+/+}$/ldlr$^{-/-}$ mice and EP4$^{-/-}$/ldlr$^{-/-}$

Table 1 Body weight and plasma lipid profile for EP4$^{+/+}$/ldlr$^{-/-}$ mice and EP4$^{-/-}$/ldlr$^{-/-}$ mice

| Animal	Duration of high fat diet (weeks)	Body weight (g)	Triglycerides (mg/dL)	Cholesterol (mg/dL)
EP4$^{+/+}$/ldlr$^{-/-}$	5	19.2 ± 0.4	260 ± 85	899 ± 99
	10	18.8 ± 0.4	182 ± 43	1233 ± 180
EP4$^{-/-}$/ldlr$^{-/-}$	5	18.8 ± 0.5	268 ± 31	1093 ± 77
	10	18.6 ± 0.3	249 ± 51	970 ± 193

Data are shown as mean $\pm$ SEM. Mice fed HFD for 5 weeks, $n = 6$; mice fed HFD for 10 weeks, $n = 7-8$.
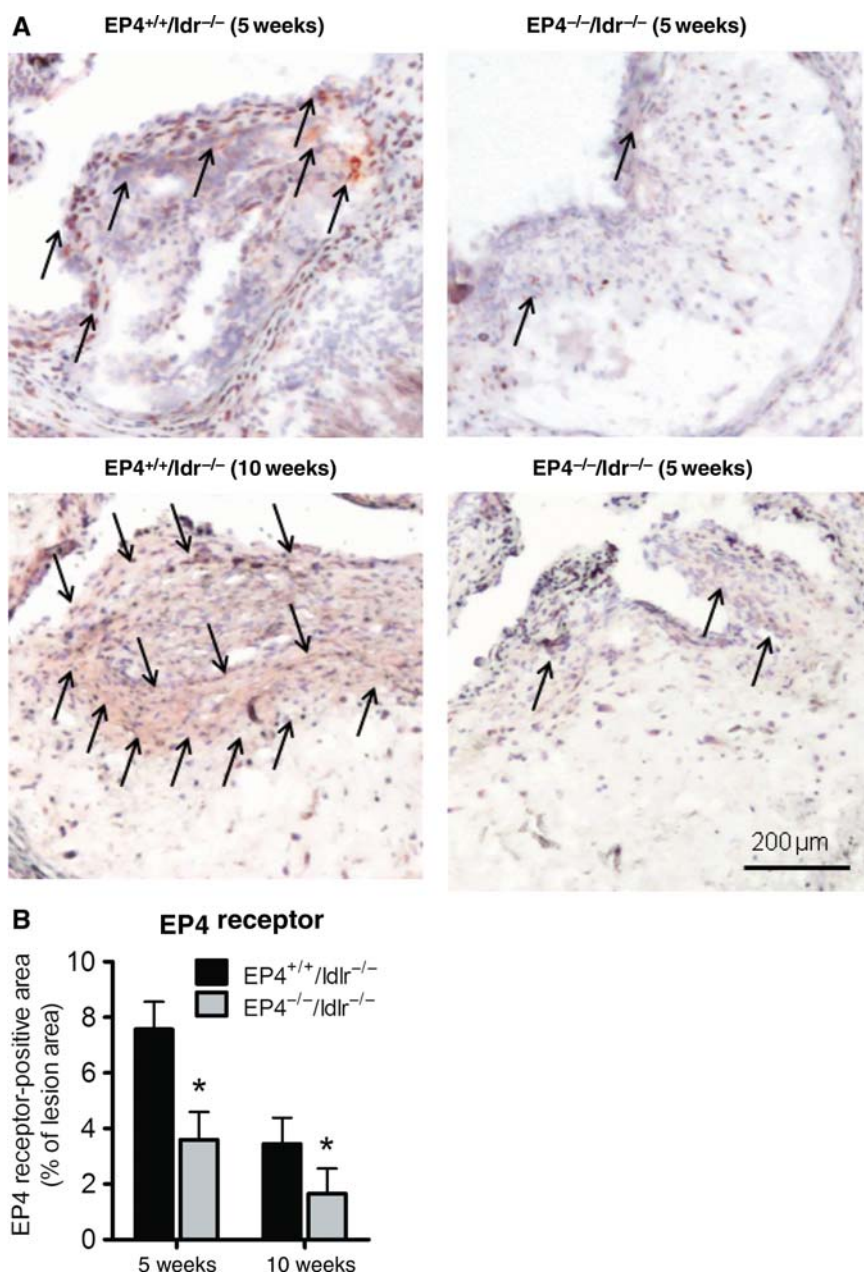
Figure 1 Representative photographs (*A*) and quantitative analysis (*B*) of EP4 staining on atherosclerotic lesions of EP4$^{+/+}$/ldlr$^{-/-}$ mice and EP4$^{-/-}$/ldlr$^{-/-}$ mice fed HFD for 5 or 10 weeks. Representative sections of aortic root lesions demonstrate EP4 localized to CD11b macrophages (*C*; top: magnification ×500, bottom: magnification ×200), CD3 T cells (*D*; magnification ×200) or α-actin SMC (*E*; top: magnification ×100; bottom; magnification ×200). Double immunofluorescent staining determined by white arrows. (*F*) Wet weight of hearts at time of sacrifice. $n = 6-8$, *$P < 0.05$ EP4$^{+/+}$/ldlr$^{-/-}$ mice vs. EP4$^{-/-}$/ldlr$^{-/-}$ mice of same duration of HFD; $^{\varphi}P < 0.05$ EP4$^{-/-}$/ldlr$^{-/-}$ mice (HFD, 5 weeks) vs. EP4$^{-/-}$/ldlr$^{-/-}$ mice (HFD, 10 weeks).

mice was 48.8 + 2.3% and 48.5 + 4.3%, respectively. Ejection fraction in the hearts of EP4$^{+/+}$/ldlr$^{-/-}$ mice and EP4$^{-/-}$/ldlr$^{-/-}$ mice was 80.5 + 2.3% and 79.1 + 4.4% at 5 weeks, and 82.1 + 2.3% and 80.9 + 1.0% at 10 weeks, respectively. Fractional shortening and ejection fraction in the hearts of EP4$^{+/+}$/ldlr$^{-/-}$ mice and EP4$^{-/-}$/ldlr$^{-/-}$ mice did not differ, at either 5 or 10 weeks of high-fat diet ($n = 6$). Thus, mice deficient of EP4 after 10 weeks of high-fat diet have oversized hearts, but they do not yet have echocardiographic signs of malfunction, suggesting that these hearts stand at the compensated stage of hypertrophy.

Lack of EP4 on bone marrow-derived cells did not affect atheroma size in mice fed a high-fat diet for 5 or 10 weeks. The amount of lipids visualized *en face* increased with the duration of high-fat diet, but no difference occurred between EP4$^{+/+}$/ldlr$^{-/-}$ mice and EP4$^{-/-}$/ldlr$^{-/-}$ mice at either time point (*Figure 2*). Lipid lesions in the aorta appeared fairly small (3.3% and 3.2% of EP4$^{+/+}$/ldlr$^{-/-}$ and EP4$^{-/-}$/ldlr$^{-/-}$ aortas, respectively, contained lipid deposits), and the majority of the lesions localized at the aortic arch, with almost no deposits along the abdominal or thoracic aorta (*Figure 2*).

Figure 1 Continued.
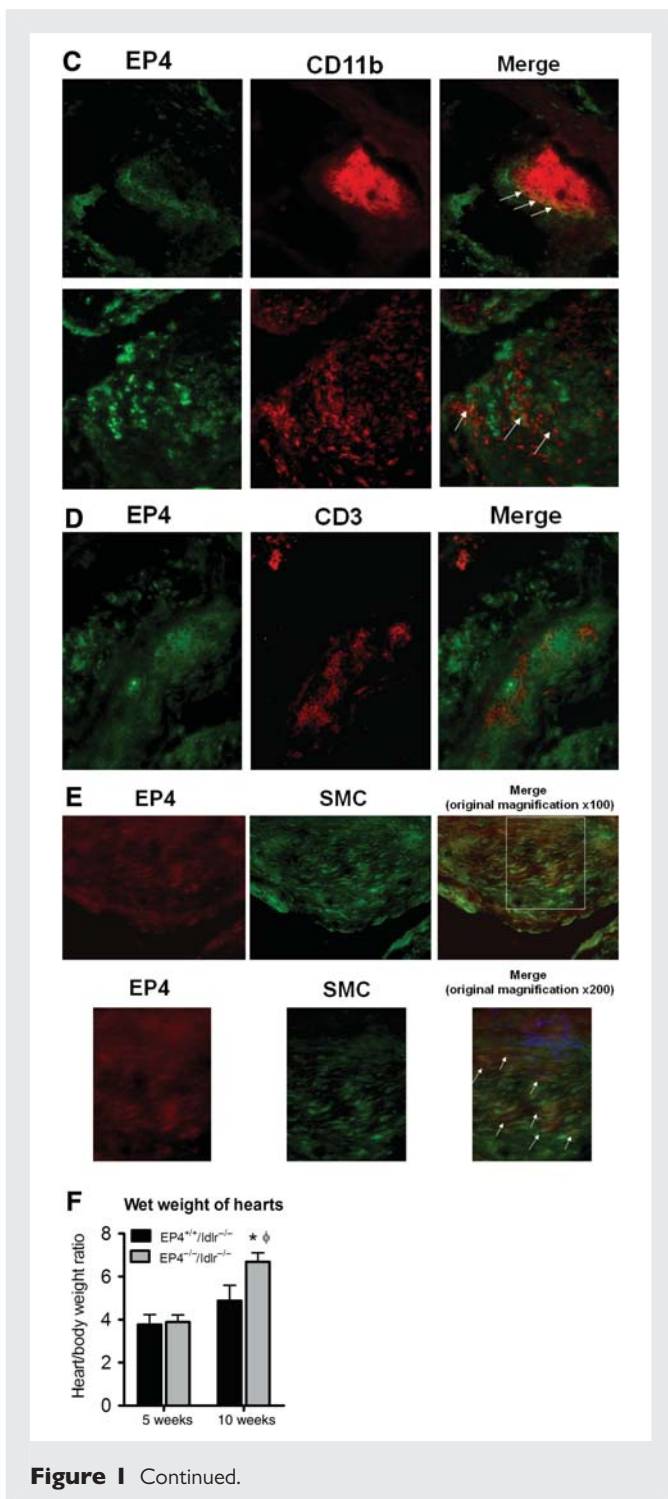
Unexpectedly, large lesions involved the aortic roots of EP4$^{+/+}$/ldlr$^{-/-}$ mice and EP4$^{-/-}$/ldlr$^{-/-}$ mice (*Figure 3*). At 5 weeks of high-fat diet, EP4$^{+/+}$/ldlr$^{-/-}$ and EP4$^{-/-}$/ldlr$^{-/-}$ mice had an average lesion area within the root (as percentage of lumen area) of 43.6% and 39.2%, respectively. Strikingly, at 10 weeks of high-fat diet, the lesion area within the root (as percentage of lumen area) reached 90.5% and 90.3% in EP4$^{+/+}$/ldlr$^{-/-}$ mice and EP4$^{-/-}$/ldlr$^{-/-}$ mice, respectively (*Figure 3A* and *B*), indicating severe stenosis at the aortic sinus. At both time points, however, the cross-section lesional areas of EP4$^{+/+}$/ldlr$^{-/-}$ and EP4$^{-/-}$/

ldlr$^{-/-}$ mice did not differ significantly (*Figure 3B*). Staining with Oil red O revealed that lipid deposits composed the bulk of the plaque (*Figure 3A* and *C*). For EP4$^{+/+}$/ldlr$^{-/-}$ or EP4$^{-/-}$/ldlr$^{-/-}$ mice at 10 weeks, lipids composed ∼35% of the lesion area, suggesting that the mice experienced an accelerated form of atherosclerosis rather than fibrosis.

Even though plaque size at the aortic roots did not differ between EP4$^{+/+}$/ldlr$^{-/-}$ and EP4$^{-/-}$/ldlr$^{-/-}$ mice at the later stage of atherosclerosis (10 weeks of high-fat diet), the cell composition and protein expression within the lesions varied substantially (*Figure 4*). At 10 weeks on a high-fat diet, the aortic root lesions of EP4$^{-/-}$/ldlr$^{-/-}$ mice had macrophage and T-cell levels 2.2-fold and 4.2-fold greater, respectively, compared with EP4$^{+/+}$/ldlr$^{-/-}$ mice (*Figure 4A*, *B*, *E*, and *F*). At 10 weeks of high-fat diet, the aortic root lesions of EP4$^{-/-}$/ldlr$^{-/}$ mice expressed MCP-1 and IP-10 2.5-fold and 1.8-fold greater, respectively, compared with EP4$^{+/+}$/ldlr$^{-/-}$ mice (*Figure 4C*, *D*, *G*, and *H*). At the 5-week time point, however, lesions of EP4$^{+/+}$/ldlr$^{-/-}$ and EP4$^{-/-}$/ldlr$^{-/-}$ mice had comparable amounts of macrophages, T cells, MCP-1, and IP-10 (*Figure 4A–H*). To extend these findings, we obtained quantitative data on mRNA encoding inflammatory mediators in extracts of the aortic roots from EP4$^{+/+}$/ldlr$^{-/-}$ and EP4$^{-/-}$/ldlr$^{-/-}$ mice fed a high-fat diet for 5 or 10 weeks by RT-PCR. At 5 weeks, EP4$^{+/+}$/ldlr$^{-/-}$ and EP4$^{-/-}$/ldlr$^{-/-}$ mice showed no difference in mRNA levels of MCP-1 or IP-10, but at 10 weeks, the expression of these chemokines was greater in EP4$^{-/-}$/ldlr$^{-/-}$ aortic root samples as compared with the wild-type counterparts (*Figure 4I* and *J*). Thoracic aorta were also used for quantitative PCR, but showed no difference in MCP-1 and IP-10 mRNA expression between EP4$^{+/+}$/ldlr$^{-/-}$ and EP4$^{-/-}$/ldlr$^{-/-}$ mice at either time point in this sample (*n* = 6; data not shown). These PCR data agree with the histological data and support our prior conclusion that EP4 leads to a decrease in chemokine expression at 10 weeks, but not at 5 weeks.

The lesions contained cells bearing markers of apoptosis, but EP4$^{+/+}$/ldlr$^{-/-}$ and EP4$^{-/-}$/ldlr$^{-/-}$ mice showed no consistent difference in apoptotic cell abundance in plaques at 5 or 10 weeks (*Figure 5A* and *C*). For quantification of SMC, the medial smooth muscle layer of the ascending aorta surrounding the lesion was not included in the analysis. We were interested in intimal smooth muscle content; therefore, only staining of α-actin within the lesion was used in the analysis. Alpha-smooth muscle positive staining localized particularly at the caps of lesions, which likely contributes to the lesional fibrous cap—comprised of macrophages and SMC—that forms during atherosclerosis. The smooth muscle content in lesions of EP4$^{+/+}$/ldlr$^{-/-}$ and EP4$^{-/-}$/ldlr$^{-/-}$ mice did not differ significantly at 5 weeks, but at 10 weeks, lesions of EP4$^{-/-}$/ldlr$^{-/-}$ mice contained significantly fewer SMC (*Figure 5B* and *D*). At 10 weeks, lesions of EP4$^{+/+}$/ldlr$^{-/-}$ and EP4$^{-/-}$/ldlr$^{-/-}$ mice had no consistent difference in MMP or cathepsin collagenolytic activity, as determined by *in situ* zymography using DQ collagen as the substrate (data not shown; *n* = 4).

4. Discussion

4.1 Allogenic bone marrow transplantation accelerated atherosclerosis

In the present study, Ldlr$^{-/-}$ mice (on a C57bL/6 background) were reconstituted with bone marrow cells from mice of a mixed
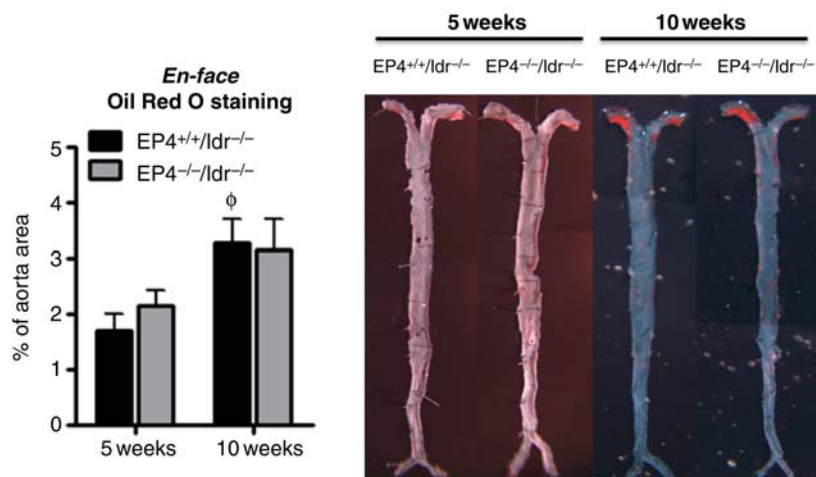
Figure 2 Representative *en face* photographs of thoracic aortas from different experimental groups stained with Oil red O (right). Quantitative analysis on the extent of atherosclerosis (expressed as percentage of lesion area to total aortic area) in thoracic aortas for all experimental groups (left). Mice fed HFD for 5 weeks, $n = 6$; mice fed HFD for 10 weeks, $n = 7-8$. $^{\varphi}P < 0.05$ EP4$^{+/+}$/ldlr$^{-/-}$ mice (HFD, 10 weeks) vs. EP4$^{+/+}$/ldlr$^{-/-}$ mice (HFD, 5 weeks).

background (129/Olac, C56bL/6, and DBA/2) to generate chimeric mice with and without EP4 in their haematopoietic lineages. Mice with targeted deletion of the EP4 gene do not survive in the congenic C57bL/6 background, but breeding mice bearing this mutation in a mixed background greatly increases survival.[17] As genetic background controls, we performed bone marrow transplantation where recipient Ldlr$^{-/-}$ mice (on a C57bL/6 background) received bone marrow cells from Ldlr$^{-/-}$ mice of the same genetic background (Ldlr$^{-/-}$/ldlr$^{-/-}$). Ldlr$^{-/-}$/ldlr$^{-/-}$ mice fed the same high-fat diet for 10 weeks had significantly smaller lesions compared with those of EP4$^{+/+}$/ldlr$^{-/-}$ mice (data not shown; $n = 8$), illustrating that allogenic bone marrow transplantation accelerated lesion formation at the aortic root. Thus, beyond the interest of this study for the role of EP4, our results provide further affirmation of the important modulatory role of cellular immunity, and in particular the allogeneic response, in atherogenesis.

The transfer of bone marrow cells from mice of non-matched genetic backgrounds itself accelerates atherosclerosis. Thus, the mechanisms of atherosclerosis in the present study may be different from those normally involved in atherosclerosis in humans or in a syngeneic Ldlr$^{-/-}$ mouse model. We previously described similar accelerated atherosclerosis formation with allogenic cardiac transplantation in rabbits.[22] Nevertheless, in the present study, bone marrow transplantation used EP4$^{-/-}$ donors and their wild-type littermates of the same mixed genetic background. All conclusions drew on the comparison of EP4$^{+/+}$/ldlr$^{-/-}$ mice vs. EP4$^{-/-}$/ldlr$^{-/-}$ mice. Thus, any difference between EP4$^{+/+}$/ldlr$^{-/-}$ mice and EP4$^{-/-}$/ldlr$^{-/-}$ mice does not result from allogenicity, but reflects the absence of EP4 on bone marrow-derived cells.

The allogenic bone marrow transplantation in our study is not completely histoincompatible. The recipient Ldlr$^{-/-}$ is of H^{2b} major histocompatibility complex (MHC) haplotypes; it received donor cells of both H^{2b} and H^{2d} MHC haplotypes. Preliminary cell proliferation assays showed there is no acute T cell proliferation during this mixed bone marrow transplantation (data not shown; $n = 3-4$), thus the occurrence of graft-vs.-host-disease (GVHD) in our chimeric

mice is unlikely. Nevertheless, we cannot eliminate the possibility of chronic GVHD as the mice continued on their high-fat diet.

4.2 EP4 deficiency enhanced local inflammation but did not alter plaque size in later atherosclerosis

This study demonstrated that mice deficient in EP4 in bone marrow-derived cells have greater expression of the T-cell chemoattractants MCP-1 and IP-10 in their aortic root lesions in late atherosclerosis (after 10 weeks of high-fat diet), compared with the wild-type counterparts. Human atheromata express these chemokines, and these mediators likely participate in leucocyte recruitment into the atheroma.[23] The lesions of EP4-deficient chimeric mice showed increased accumulation of macrophages and T cells, indicating an escalation of local inflammation. These findings support a role for EP4 as an anti-inflammatory mediator in atherogenesis *in vivo*. Serum triglyceride and cholesterol did not differ between the two experimental groups, suggesting that the enhanced inflammation stems from the absence of EP4 on bone marrow-derived cells.

Despite the marked difference in chemokine expression and amount of inflammatory cells between the lesions of EP4$^{+/+}$/ldlr$^{-/-}$ and EP4$^{-/-}$/ldlr$^{-/-}$ mice, lesion burden did not differ at the aortic sinus or at the aorta between the two experimental groups. However, the large plaque sizes formed at the aortic roots of mice that consumed a high-fat diet for only 10 weeks intrigued us. Cross-sectional lesion area of the aortic roots (expressed in percentage of lumen area) averaged to 90.5% and 90.3% in EP4$^{+/+}$/ldlr$^{-/-}$ and EP4$^{-/-}$/ldlr$^{-/-}$ mice, respectively, yielding subtotal occlusion of the aortic root. The finding of functional supravalvular aortic stenosis could well have caused the premature death observed after 8–10 weeks of high-fat diet in our experimental mice. Conversely, the plaques in the descending aortas appeared very modest in size. EP4$^{+/+}$/ldlr$^{-/-}$ and EP4$^{-/-}$/ldlr$^{-/-}$ mice had lesional area on aortas (expressed in percentage of total aortic area) of only 3.3% and 3.2%, respectively. The different rates in atherosclerosis development between the aorta and the aortic sinus could result from the hydrodynamic differences in these two regions.
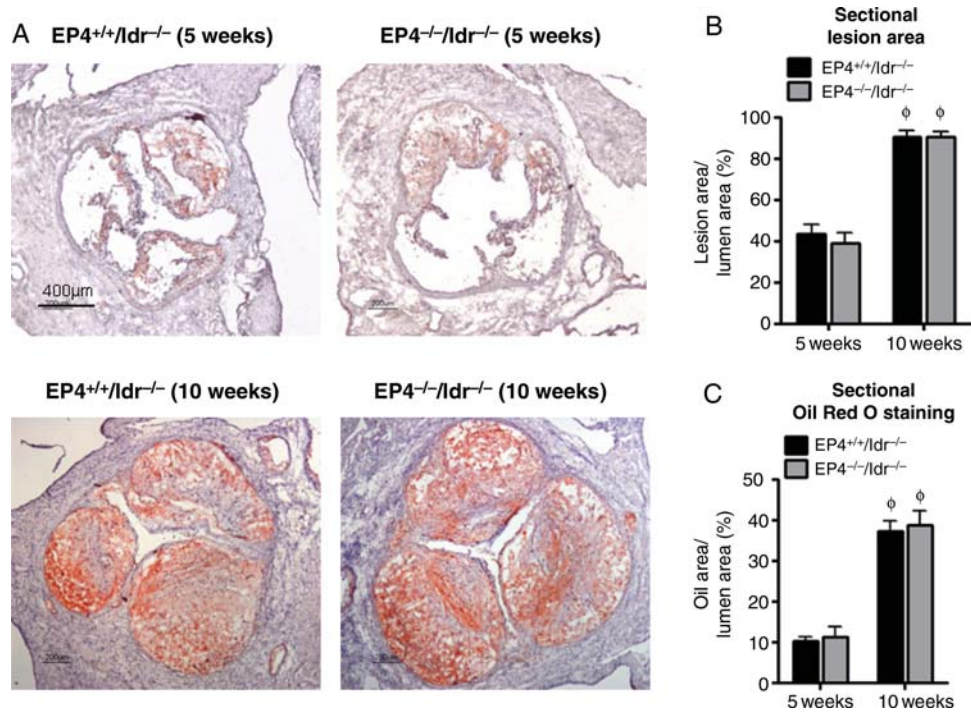
Figure 3 Effects of EP4 deletion on lesion morphology. (*A*) Oil Red O staining on representative atherosclerotic lesions from EP4^{+/+}/ldlr^{−/−} mice and EP4^{−/−}/ldlr^{−/−} mice fed HFD for 5 or 10 weeks. Quantitative analysis of lesion area (*B*), Oil Red O positive staining (*C*) on atherosclerotic aortic root lesion of EP4^{+/+}/ldlr^{−/−} mice and EP4^{−/−}/ldlr^{−/−} mice fed HFD for 5 or 10 weeks. $n = 6–8$, [φ]$P < 0.05$ EP4^{−/−}/ldlr^{−/−} mice or EP4^{−/−}/ldlr^{−/−} mice fed HFD (5 weeks) vs. HFD (10 weeks).

Radiation compromises the endothelial function at the aorta and the aortic sinus, but the latter region experiences highly disturbed hemodynamic flow, which advances atherosclerosis development.[24] Schiller *et al.* (2001)[25] described similar disproportional plaque formation among different locations, and demonstrated that irradiation and syngeneic bone marrow reconstitution exacerbated atherosclerosis within the aortic root and, interestingly, inhibited lesion progression across the surface of the aorta. In these experiments, the partial histocompatibility mismatch mandated by the postnatal lethality of EP4 deficiency on a congenic background may have further exaggerated lesion formation in the aortic root.

4.3 EP4 deficiency does not affect inflammation or plaque size in less mature atheromata

Plaque size at the aortic root did not differ between EP4^{+/+}/ldlr^{−/−} and EP4^{−/−}/ldlr^{−/−} mice after 10 weeks of high-fat diet. Owing to the formation of large lesions, we speculated whether lesion progression would plateau at this late time point, hence masking any true differences in lesion size between the two groups of mice. To explore this possibility, we repeated the study with a shorter high-fat feeding regimen of 5 weeks. At 5 weeks of high-fat diet, deficiency of EP4 did not alter MCP-1 and IP-10 expression as it did at 10 weeks, nor did it affect macrophage and T-cell infiltration within the lesions. These findings suggest that EP4^{+/+}/ldlr^{−/−} and EP4^{−/−}/ldlr^{−/−} mice had similar severity of inflammation in early atherosclerosis, and that the EP4-dependent anti-inflammatory effect only becomes manifest in later atherosclerosis. EP4^{+/+}/ldlr^{−/−} and EP4^{−/−}/ldlr^{−/−} mice had comparable plaque burden in the aorta and lesion size at the root after 5 weeks of high-fat diet. Thus, deficiency of EP4 on bone marrow-derived cells does not modify lesion size either at earlier or later stages of atherosclerosis.

4.3.1 EP4 and apoptosis
In contrast to the findings of Babaev *et al.*,[12] the number of apoptotic cells did not differ between the aortic root lesions of EP4^{+/+}/ldlr^{−/−} and EP4^{−/−}/ldlr^{−/−} mice in our experiment, either after 5 or 10 weeks of high-fat diet. The discrepancy in the results could result from differences in experimental design. Mice in the study by Babaev *et al.* consumed an atherogenic diet for 8 weeks, while mice in our study ate a Western diet for either 5 or 10 weeks. Our study consists of allogenic bone marrow transplantation that accelerated atherosclerosis; thus, in absolute terms, the high-fat diet lasted only 5 weeks, but it probably represents a more advanced stage of atherosclerosis than in the mice fed for 8 weeks in the study by Babaev *et al.* Moreover, their study focused on apoptosis and its effect on early-phase atherosclerosis, whereas our study examined the role of apoptosis at late phases of the disease. Babaev *et al.* specifically investigated the role of EP4 in apoptosis, but did not examine the effect of EP4 on inflammation or other mechanisms related to atherosclerosis. Taken together, these studies suggest that EP4 may suppress macrophage apoptosis and enhance formation of atherosclerosis at the early phase of the disease, but it does not modulate apoptosis or plaque formation at later phases of the disease.
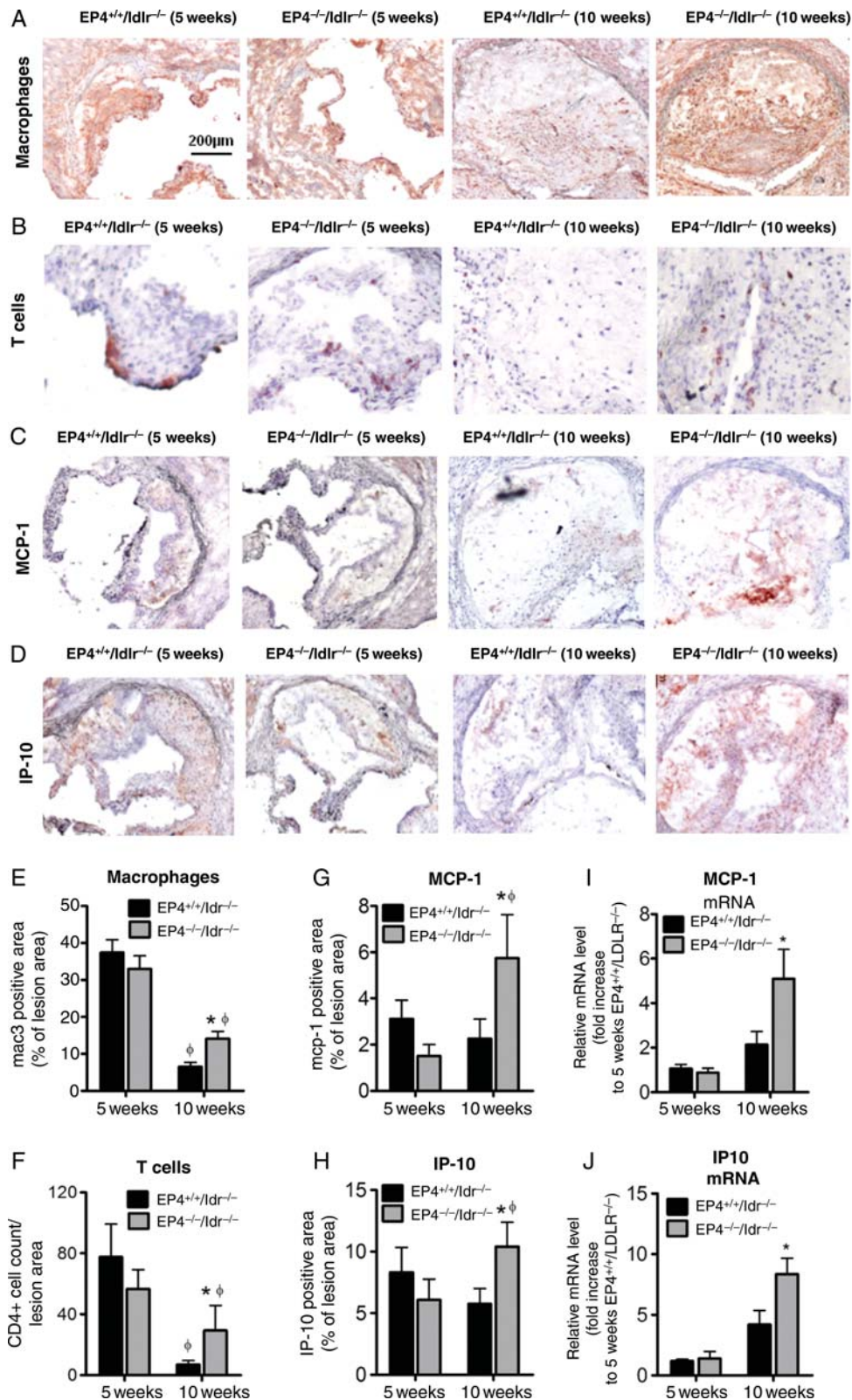
Figure 4 Lesional sections were stained for mac-3 (*A*), CD4 (*B*), MCP-1 (*C*), and IP-10 (*D*) to detect macrophages, T cells, and two chemokines, respectively. All positive staining is reflected by reddish-brown color. Quantitative analysis for macrophages (*E*), T cells (*F*), MCP-1 (*G*), and IP-10 (*H*) are shown at the lower panel. $n = 6$–8, *$P < 0.05$ EP4$^{+/+}$/ldlr$^{-/-}$ mice vs. EP4$^{-/-}$/ldlr$^{-/-}$ mice of same duration of HFD; $^{\varphi}P < 0.05$ EP4$^{-/-}$/ldlr$^{-/-}$ mice or EP4$^{-/-}$/ldlr$^{-/-}$ mice fed HFD (5 weeks) vs. HFD (10 weeks). Quantitative RT-PCR analysis of MCP-1 (I) and IP-10 (J) in aortic root samples of EP4$^{+/+}$/ldlr$^{-/-}$ mice vs. EP4$^{-/-}$/ldlr$^{-/-}$ mice fed HFD for 5 or 10 weeks. Expression of MCP-1 and IP-10 was quantitated relative to EP4$^{+/+}$/ldlr$^{-/-}$ mice fed HFD (5 weeks) and corrected for expression of β-actin. Values shown are means $\pm$ SEM. *$P < 0.05$ vs. EP4$^{+/+}$/ldlr$^{-/-}$ mice fed HFD (10 weeks).
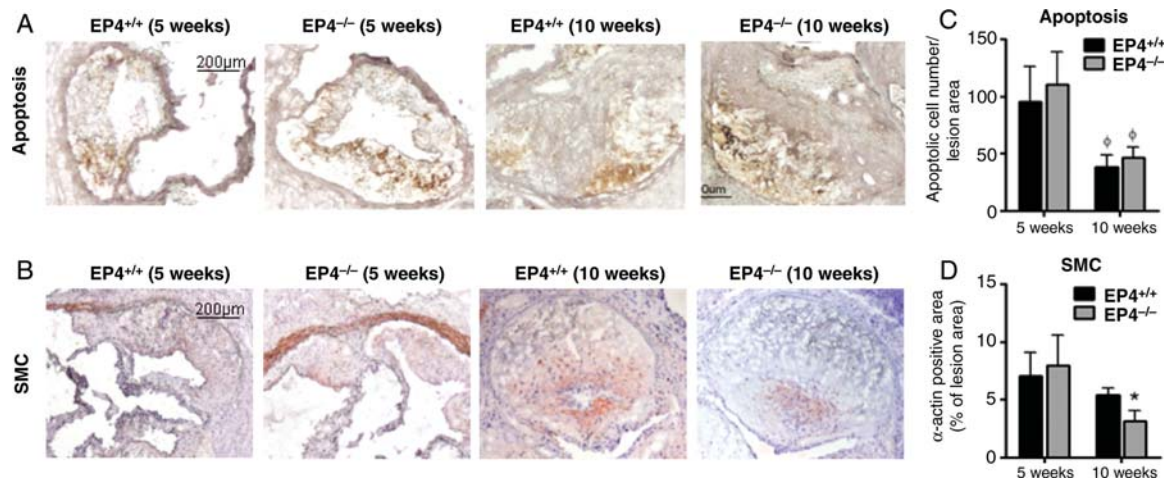
Figure 5 Lesion sections were stained for apoptotic markers (*A*) and α-actin (*B*) to detect apoptotic cells and SMC, respectively. Quantitative analysis for apoptosis and SMC at the lower panel. $n = 6-8$, *$P < 0.05$ EP4$^{+/+}$/ldlr$^{-/-}$ mice vs. EP4$^{-/-}$/ldlr$^{-/-}$ mice of same duration of HFD; $^{\varphi}P < 0.05$ EP4$^{-/-}$/ldlr$^{-/-}$ mice or EP4$^{-/-}$/ldlr$^{-/-}$ mice fed HFD (5 weeks) vs. HFD (10 weeks).
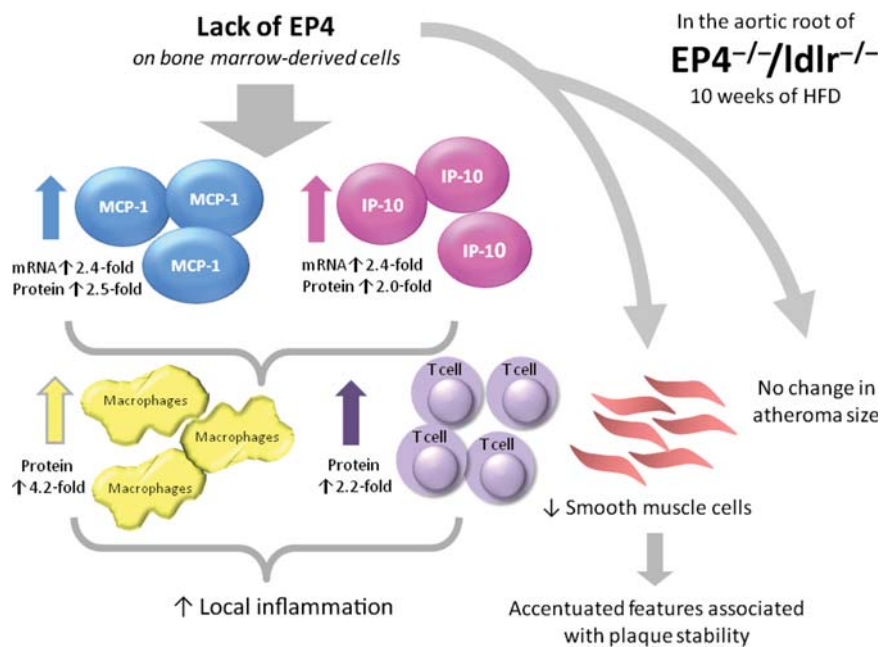
Figure 6 Schema of the major results and interpretation of this study. After 10 weeks of high-fat diet, EP4-deficient chimeric mice displayed enhanced inflammation in their atherosclerotic plaques. Expression of MCP-1 and IP-10 increased, along with a corresponding increase in macrophage and T-cell infiltration. These plaques also exhibited fewer SMC—a character of vulnerable plaques—but EP4 deficiency had no effect on plaque size.

4.3.2 EP4 and proteolytic enzymes

In addition to affecting inflammation and apoptosis, PGE$_2$ may impact the development and fate of atherosclerotic plaques by altering the activity of proteolytic enzymes. The aortic root lesions of EP4$^{+/+}$/ldlr$^{-/-}$ and EP4$^{-/-}$/ldlr$^{-/-}$ mice had no detectable difference in collagenolytic MMP activity in our study. We also investigated the activity of cysteinyl cathepsins (another major class of protease involved an atherosclerosis) within the aortic lesions.[26] Our results show no difference in the cathepsin activity between lesions of EP4$^{+/+}$/ldlr$^{-/-}$ and EP4$^{-/-}$/ldlr$^{-/-}$ mice. Hence, despite the number of *in vitro* and

in vivo studies suggesting a role of EP4 in regulating proteases under various pathophysiological settings,[27–30] these *in vivo* experiments showed no obvious change in arterial protease activity dependent on EP4.

4.3.3 EP4 deficiency modulates SMC

SMC produce fibrous proteins that are implicated in plaque stability. On the other hand, lesional macrophages produce proteases that can degrade the plaque's extracellular matrix, favouring formation of plaques considered prone to rupture in humans. The rate of matrix

degradation potential, as determined by collagenolytic activity, did not differ between EP4$^{+/+}$/ldlr$^{-/-}$ and EP4$^{-/-}$/ldlr$^{-/-}$ mice, despite a divergence in macrophage numbers. But the fewer SMC residing in the caps of the plaques of EP4$^{-/-}$/ldlr$^{-/-}$ mice high-fat fed for 10 weeks suggest that the lack of EP4 results in plaques that are more vulnerable to rupture (*Figure 6*).

5. Conclusion

Targeting EP4 in treating cardiovascular diseases recently has garnered interest, with reports of the role of EP4 receptor and the benefits of EP4 agonist in preventing acute cardiac rejection in allograft transplants, ischaemic injury of myocardium reperfusion, and the development of abdominal aortic aneurysm. This study investigated the role of EP4 in atherosclerosis *in vivo*, and particularly its effect on inflammation. The presence of EP4 on bone marrow-derived cells has little effect on plaque size or morphology at early stages of atherosclerosis, but at later stages of atherosclerosis, the presence of EP4 receptor dampened local inflammation (reduced expression of chemotactic proteins, including MCP-1 and IP10; and reduced inflammatory cells, such as macrophages and T cells) and increased SMC within the plaque. But this interference in EP4 function did not prevent progression of atherosclerosis or alter lesion size in the aorta or at the aortic root. Moreover, the presence of EP4 did not impact apoptosis or collagenase activity during the pathogenesis of atherosclerosis. Accumulating studies suggest that asymptomatic and symptomatic lesions differ with regard to inflammatory burden rather than plaque size. As we enter an era that sees growing interest in developing drugs that affect plaque biology, not just bulk, EP4 may serve as an attractive therapeutic target to suppress inflammation in established atheromata.

References

1. Sugimoto Y, Narumiya S. Prostaglandin E receptors. *J Biol Chem* 2007;**282**: 11613–11617.
2. Takayama K, Garcia-Cardena G, Sukhova G, Comander J, Gimbrone MA, Libby P. Prostaglandin E$_2$ suppresses chemokine production in human macrophages through the EP4 receptor. *J Biol Chem* 2002;**277**:44147–44154.
3. Minami M, Shimizu K, Okamoto Y, Folco E, Ilasaca ML, Feinberg MW *et al*. Prostaglandin E receptor type 4-associated protein interacts directly with NF-kappaB1 and attenuates macrophage activation. *J Biol Chem* 2008;**183**:9692–9703.
4. Regan JW. EP2 and EP4 prostanoid receptor signaling. *Life Sci* 2003;**74**:143–153.
5. Takayama K, Sukhova GK, Chin MT, Libby P. A novel prostaglandin E receptor 4-associated protein participates in anti-inflammatory signaling. *Circ Res* 2006;**98**: 499–504.
6. Ogawa M, Suzuki J, Kosuge H, Takayama K, Nagai R, Isobe M. The mechanism of anti-inflammatory effects of prostaglandin E$_2$ receptor 4 activation in murine cardiac transplantation. *Transplantation* 2009;**87**:1645–1653.
7. Hishikari K, Suzuki J, Ogawa M, Isobe K, Takahashi T, Onishi M *et al*. Pharmacological activation of the prostaglandin E$_2$ receptor EP4 improves cardiac function after myocardial ischaemia/reperfusion injury. *Cardiovasc Res* 2009;**81**:123–132.
8. Xiao CY, Yuhki K, Hara A, Fujino T, Kuriyama S, Yamada T *et al*. Prostaglandin E$_2$ protects the heart from ischemia-reperfusion injury via its receptor subtype EP$_4$. *Circulation* 2004;**109**:2462–2468.
9. Tang EHC, Shvartz E, Sukhova G, Shimizu K, Shi GP, Zheng C *et al*. Deletion of EP4 receptors on bone marrow-derived cells enhances inflammation and angiotensin II-induced abdominal aortic aneurysm formation. 2009; (submitted for publication).
10. Cipollone F, Prontera C, Pini B, Marini M, fazia M, Cesare DD *et al*. Overexpression of functionally coupled cyclooxygenase-2 and prostaglandin E synthase in symptomatic atherosclerotic plaques as a basis of prostaglandin E$_2$-dependent plaque instability. *Circulation* 2001;**104**:921–927.
11. Cipollone F, Fazia ML, Iezzi A, Cuccurullo C, De Cesare D, Ucchino S *et al*. Association between prostaglandin E receptor subtype EP4 overexpression and unstable phenotype in atherosclerotic plaques in human. *Arterioscler Thromb Vasc Biol* 2005;**9**: 1925–1931.
12. Babaev VR, Chew JD, Ding L, Davis S, Breyer MD, Breyer RM *et al*. Macrophages EP4 deficiency increases apoptosis and suppresses early atherosclerosis. *Cell Metab* 2008; **8**:492–501.
13. Geng YJ, Libby P. Progression of atheroma: a struggle between death and procreation. *Arterioscler Thromb Vasc Biol* 2002;**22**:1370–1380.
14. Tabas I. Apoptosis and efferocytosis in mouse models of atherosclerosis. *Curr Drug Targets* 2007;**8**:1288–1296.
15. Seimon T, Tabas I. Mechanisms and consequences of macrophage apoptosis in atherosclerosis. *J Lipid Res* 2009;**50**:S382–S387.
16. Sanghi S, MacLaughlin EJ, Jewell CW, Chaffer S, Naus PJ, Watson LE *et al*. Cyclooxygenase-2 inhibitors: a painful lesson. *Cardiovasc Hematol Disord Drug Targets* 2006;**6**:85–100.
17. Nguyen M, Camenisch T, Snouwaert JN, Hicks E, Coffman TM, Anderson PA *et al*. The prostaglandin receptor EP4 triggers remodeling of the cardiovascular system at birth. *Nature* 1997;**390**:78–91.
18. Fukuda D, Sata M, Ishizaka N, Nagai R. Critical role of bone marrow angiotensin II type 1 receptor in the pathogenesis of atherosclerosis in apolipoprotein E deficient mice. *Arterioscler Thromb Vasc Biol* 2008;**28**:90–96.
19. Sukhova GK, Zhang Y, Pan JH, Wada Y, Yamamoto T, Naito M *et al*. Deficiency of cathepsin S reduces atherosclerosis in LDL receptor-deficient mice. *J Clin Invest* 2003;**111**:897–906.
20. Sun J, Sukhova G, Yang M, Wolters PJ, MacFarlane LA, Libby P *et al*. Mast cells modulate the pathogenesis of elastase-induced abdominal aortic aneurysms in mice. *J Clin Invest* 2007;**117**:3359–3368.
21. Schneider F, Sukhova GK, Aikawa M, Canner J, Gerdes N, Tang SM *et al*. Matrix-metalloproteinase-14 deficiency in bone-marrow-derived cells promotes collagen accumulation in mouse atherosclerotic plaques. *Circulation* 2008;**117**: 931–939.
22. Tanaka H, Sukhova GK, Libby P. Interaction of the allogeneic state and hypercholesterolemia in arterial lesion formation in experimental cardiac allografts. *Arterioscler Thromb Vasc Biol* 1994;**14**:734–745.
23. Braunersreuther V, Mach F, Steffens S. The specific role of chemokines in atherosclerosis. *Thromb Haemost* 2007;**97**:714–721.
24. Gimbrone MA Jr, Topper JN, Nagel T, Anderson KR, Garcia-Cardeña G. Endothelial dysfunction, hemodynamic forces and atherogenesis. *Ann N Y Acad Sci* 2000;**902**: 230–239.
25. Schiller NK, Kubo N, Boisvert WA, Curtiss LK. Effect of gamma-irradiation and bone marrow transplantation on atherosclerosis in LDL receptor-deficient mice. *Arterioscler Thromb Vasc Biol* 2001;**21**:1674–1680.
26. Liu J, Sukhova GK, Sun JS, Xu WH, Libby P, Shi GP. Lysosomal cysteine proteases in atherosclerosis. *Arterioscler Thromb Vasc Biol* 2004;**24**:1359–1366.
27. Ruwanpura SM, Noguchi K, Ishikawa I. Prostaglandin E2 regulates interleukin-1beta-induced matrix metalloproteinase-3 production in human gingival fibroblasts. *J Dent Res* 2004;**83**:260–265.
28. Pavlovic S, Du B, Sakamoto K, Khan KMF, Natarajan C, Breyer RM *et al*. Targeting prostaglandin E$_2$ receptors as an alternative strategy to block cyclooxygenase-2-dependent extracellular matrix-induced matrix metalloproteinase-9 expression by macrophages. *J Biol Chem* 2006;**281**:3321–3328.
29. Wu MH, Shoji Y, Wu MG, Chuang PC, Lin CC, Huang MF *et al*. Suppression of matrix metalloproteinase-9 by prostaglandin E$_2$ in peritoneal macrophage is associated with severity of endometriosis. *Am J Pathol* 2005;**67**:1061–1069.
30. Yan M, Noguchi K, Ruwanpura SM, Ishikawa I. Cyclooxygenase-2-dependent prostaglandin (PG) E2 downregulates matrix metalloproteinase-3 production via EP2/EP4 subtypes of PGE2 receptors in human periodontal ligament cells stimulated with interleukin-1alpha. *J Periodontol* 2005;**76**:929–935.